Acta Cryst. (1990). A**46**, 923-929

Diffraction Effect of X-ray Diffuse Scattering in a Disordered Cu–Al Alloy

BY MASAHIRO MORI, YASUJI KASHIWASE AND MOTOKAZU KOGISO

Department of Physics, College of General Education, Nagoya University, Chikusa, Nagoya 464, *Japan*

AND SATOSHI SASAKI

Photon Factory, National Laboratory for High Energy Physics, Tsukuba, Ibaraki 305, *Japan*

(*Received* 24 *August* 1989; *accepted* 27 *June* 1990)

Abstract

A white (defect) line which appears as a dip in intensity distribution was clearly observed in the 200 diffuse scattering from a Cu–Al disordered crystal at room temperature in the Bragg geometry by using both photographic and counter methods. The line is caused by the extinction effect on the 200 Bragg reflection, subsequent to the diffuse scattering, in a process similar to the case of mosaic crystals. The diffuse scattering is caused by the static displacement as well as the thermal motion of atoms. The observed contrast of the line is quantitatively in fair agreement with that calculated.

Introduction

Dynamical diffraction effects associated with thermally scattered X-rays in a crystal were predicted theoretically by Kainuma (1955, 1961) to be similar to the case of Kikuchi lines and bands in electron diffraction. Recently, Kashiwase, Mori, Kogiso, Minoura & Sasaki (1988) observed diffraction lines on diffraction photographs of the thermal diffuse scattering (TDS) near the reciprocal-lattice point of a perfect germanium crystal in the Laue (transmission) geometry. The diffraction lines appeared as black or black-white lines, which were called excess or excess-defect lines, respectively, according to experimental conditions. The authors also observed a pair of excess lines (EL) near a reciprocal-lattice point and the incident-beam spot. Quantitative measurement was further carried out in some detail using monochromatized synchrotron radiation and a triple-crystal diffractometer. The excess line was thereby reasonably explained by the anomalous transmission of TDS X-rays caused by dynamical diffraction and absorption in perfect crystals (Kashiwase, Mori, Kogiso, Ushida, Minoura, Ishikawa & Sasaki, 1989).

In the case of mosaic crystals, Kashiwase, Kainuma & Minoura (1981, 1982) observed white lines, which they called defect lines (DL) across X-ray TDS spots near the low-order reciprocal-lattice points of crystals such as urea nitrate and pyrolytic graphite. They attributed the DL to the Bragg reflection of TDS as determined from the experimental crystal orientation dependence. Similar phenomena were observed for LiF crystals by Bushuev, Laushkin, Kuz'min & Lobanov (1983) and Bushuev & Lyubimov (1987). They developed a diffraction theory of inelastically scattered X-rays including TDS in practical mosaic crystals on the basis of the theory of secondary extinction by Hamilton (1957) and Zachariasen (1967). They showed that the contrast and the angular width of the diffraction line depend on the degree of perfection of mosaic crystals. Applying their theory, Oya & Kashiwase (1988) also quantitatively explained the contrast and the width of the DL from a pentaerythritol crystal in both Laue and Bragg (reflection) geometries.

The previous experiments were, however, made only in crystallographically good crystals with nearly periodic structure. Nothing was reported about the diffraction effect of X-ray diffuse scattering in crystals with local disorder. In order to study the diffraction effect in such a non-perfect case, we chose a Cu–Al solid-solution (disordered f.c.c.) crystal as a specimen. The reasons are as follows. Single crystals with a reasonably small mosaic spread can be prepared in spite of the solid-solution crystal growth. The existence of diffuse scattering due to local order is well known in this alloy (Epperson, Fürnrohr & Ortiz, 1978); Cu and Al atoms are substantially different in scattering amplitude and atomic size; the effect of the surface roughness is expected to be small since the X-ray penetration depth is appreciable for the component elements.

In a solid-solution crystal, there are three kinds of X-ray diffuse scattering (Warren, 1969). The first is TDS. The second is associated with the atom size disparity and is referred to as the size-effect modulation and the Huang scattering. These occur because, in the disordered solid solution, there are static displacements from the exact (average) f.c.c. lattice positions depending on whether a site is occupied by a Cu an Al atom. The third contribution is the diffuse scattering of the short-range-order (SRO) fluctuations in the Cu–Al solid-solution crystal. Since this scattering intensity, due to SRO, is usually much weaker near the Bragg reflection point than the TDS intensity,

0108-7673/90/110923-07$03.00

this contribution presumably has no serious effect on the aim of this experiment.

The principal purpose of this study is to observe a diffraction effect, that is, sharp diffraction lines due to the above-mentioned diffuse scattering in the solid-solution crystal. The diffraction lines of the diffuse scattering, including TDS, is distinguishable from those of other inelastically scattered X-rays. The intensity of the diffuse scattering depends strongly on the crystal orientation while the intensity of inelastically scattered X-rays produced through fluorescence and Compton scattering is not sensitive to orientation. The diffuse scattering is also quasi-elastic, as the energy change of the TDS X-ray is equal to the creation or annihilation energy of a phonon, while the energy change in diffuse scattering due to size effect or SRO is essentially zero. Compton scattered X-rays near a low-order Bragg spot are expected to produce a diffraction line at a higher angle by a few tenths of a degree than the elastic or quasi-elastic X-rays. The effect of fluorescent X-rays can be eliminated by using the monochromatic Cu $K\alpha$ line, since the strongest fluorescence from the present Cu-rich specimen would be Cu $K\alpha$.

Experimental methods and results

Large single crystals of a f.c.c. Cu-Al alloy were grown in graphite crucibles with the Bridgman method and homogenized by annealing for two days at 970 K. The purities of both initial materials were better than 99·99%. The atomic ratio of copper and aluminium is 86:14, which is the maximum concentration of aluminium to get large crystals of the f.c.c. phase. After slicing with a diamond cutter, the single-crystal faces were polished flat with emery papers. Then they were chemically polished with a solution of 50% HNO_3, 25% H_3PO_4 and 25% acetic acid. The sample surface was normal to [100] within 2°. The typical size of the sample was $5\times10\times0{\cdot}15$mm.

To check the degree of crystal perfection, we observed the half-width at half-maximum (HWHM = $\Delta\theta_B$) of the ω-scan intensity profile of the 200 Bragg reflection with Cu $K\alpha_1$. The values of the HWHM were 1·5–5′. Of greatest importance was to choose a sample in which the 200 reflection forms a simple single peak. The final sample perfection is clearly denoted by the sharp and small Bragg spots in Fig. 1.

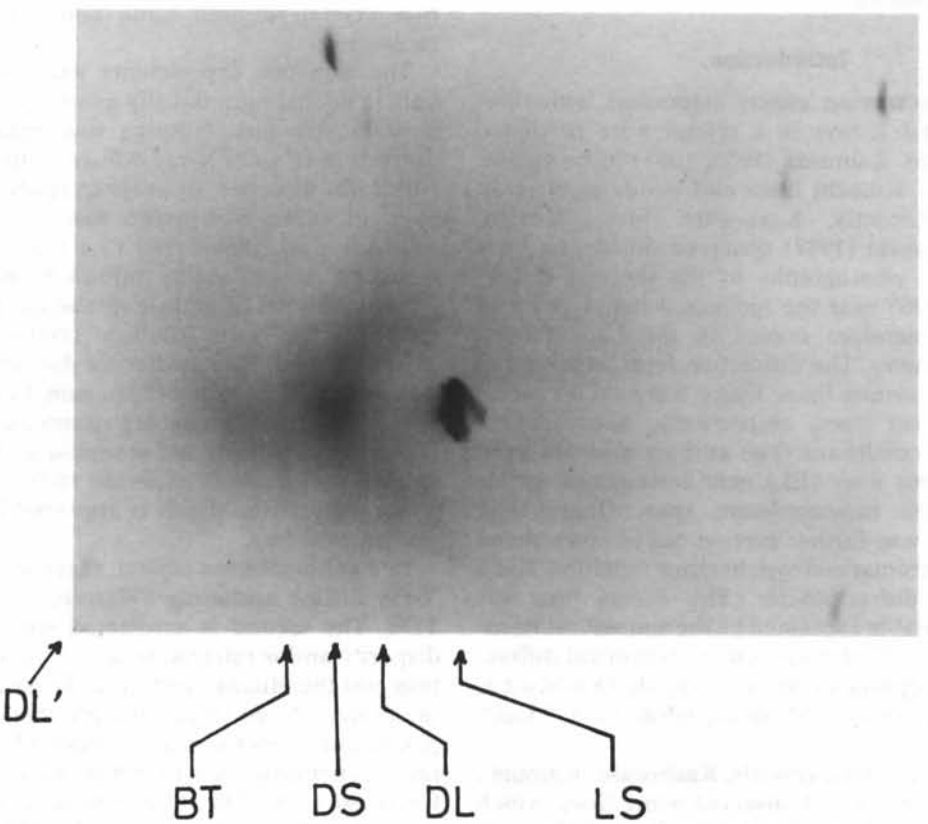

Fig. 1. Diffraction photograph of the Cu-Al alloy taken for $\Delta\omega = 3°$, indicating DL, white line; DS, intensity maximum point of diffuse scattering; BT, tail of the 200 Bragg reflection with Cu $K\alpha$ X-rays and LS, the Laue spot due to white radiation. DL′ shows perhaps the diffraction effect associated with another reciprocal-lattice point.

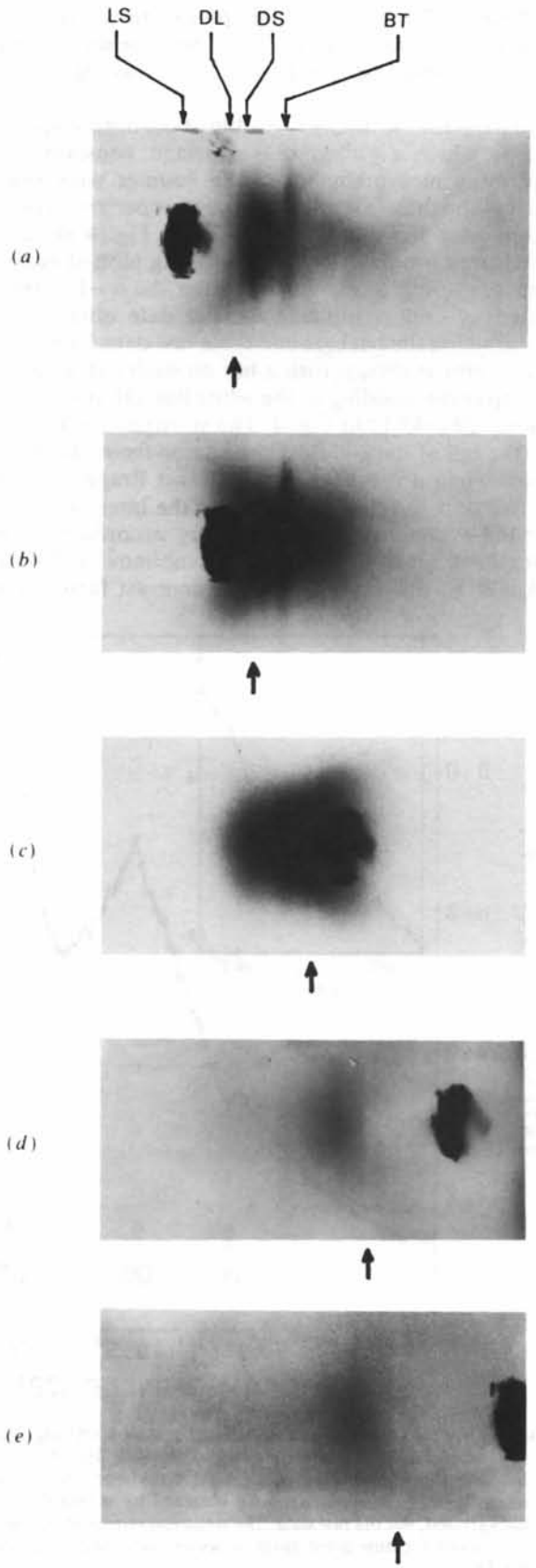

This photograph, which will be discussed below, is a back-Laue photograph taken for the sample rotated by +3 ° off the exact 200 Bragg position for Cu $K\alpha$ X-rays.

An X-ray generator with a Philips fine-focus Cu anode X-ray tube was used at 45 kV and 25 mA. All experiments were carried out by rotation around the [001] axis of the specimen at room temperature in the Bragg geometry. We used SCRE, Sakura cosmic-ray film, for high-sensitive X-ray films. The Ni-filtered X-ray beam was collimated with a tube of length 60 mm and a hole diameter 0·5 mm. The use of an Ni filter was essential to avoid the strong Cu fluorescence. A part of the experiment was also made using the 1·540 Å monochromatized synchrotron radiation.

Firstly, diffraction photographs were taken for the crystal set at various orientations to observe the diffraction effect of diffuse scattering. The dimensions of the arrangement were 140 mm between X-ray source and sample, and 100 mm between sample and film. The exposure times were 1–400 h. The DL in the photographs was detectable within $|\Delta\omega| = 10\,°$. Here, we have introduced the notation $\Delta\omega = 90\,° - \psi - \theta_B$ in which ψ and θ_B are the glancing and 200 Bragg reflection angles shown in Fig. 3. Fig. 1 shows a photograph taken for $\Delta\omega = 3\,°$. The clear spot LS is the Laue spot due to the 200 (mirror) reflection of weak white X-rays. DS indicates the maximum-intensity position of diffuse scattering for Cu $K\alpha$ X-rays near the 200 reciprocal-lattice point. BT refers to the tail of the 200 Bragg reflection due to Cu $K\alpha$. The angle between BT and the incident beam (IB) is always equal to $2\theta_B$. The long white line DL can be seen midway between LS and BT. The DL is extremely long compared with the DL of TDS in the previous observations (for example, Kashiwase *et al.*, 1982). From the above experiment, it cannot be clarified whether the DL was caused only by the diffraction effect of diffuse scattering. We can also see a long weaker DL (DL′), which may be the diffraction effect associated with another reciprocal-lattice point, from top of center to lower left-hand corner in Fig. 1.

Further experiments were made to get detailed aspects of the DL under higher angular resolution. The sample-film distance was about 400 mm and the exposure times were 10–200 h. Figs. 2(*a*)–(*e*) show the diffraction photographs taken with the angles $\Delta\omega = -1{\cdot}3$, $-0{\cdot}8$, $0{\cdot}7$, $2{\cdot}0$ and $2{\cdot}7\,°$, respectively. These photographs can be explained as shown in Fig. 1. A long white DL can be observed at the middle point between LS and BT. From these photographs we can see the ω dependence of DL. The contrast of the DL decreases with increasing $|\Delta\omega|$, along with

Fig. 2. Diffraction photographs of the Cu–Al alloy for various crystal orientations in the Bragg geometry. The white line, DL, in each photograph is indicated by an arrow. (*a*) $\Delta\omega = -1{\cdot}3\,°$, (*b*) $\Delta\omega = -0{\cdot}8\,°$, (*c*) $\Delta\omega = 0{\cdot}7\,°$, (*d*) $\Delta\omega = 2{\cdot}0\,°$, (*e*) $\Delta\omega = 2{\cdot}7\,°$.

reduction of the diffuse scattering intensity. Hence, the origin of DL is attributed to diffuse scattering, and not to the other X-ray (inelastic) scattering processes. It seems that the cause of the remarkably long DL in Fig. 1 is not only the TDS, but also the diffuse scattering produced by the static displacement of atoms.

The diffraction geometry of the white line DL is shown schematically in Fig. 3. The diffuse scattering which satisfies the Bragg condition will be reflected in the direction of EL with the deviation angle $2\theta_B$ from EL and it turns out to be the white line DL. We define 2Ψ as the angle of the propagating direction of DL from the incident beam IB, and $\Delta(2\Psi)$ as the deviation from $2\theta_B$. When the sample is rotated, the DL moves, satisfying the relation

$$\Delta(2\Psi) = \Delta\omega,$$

which coincides with the fact that DL always lies in the middle of LS and BT. This fact also shows that the origin of the DL is not Compton scattering but, rather, diffuse scattering. Near the Bragg reflection point, 'incoherent' scattering and diffuse scattering due to SRO are much weaker than the Huang diffuse scattering and TDS. We did not try to observe the black line, the excess line (EL), near the strong incident beam (IB).

A quantitative measurement was performed to investigate the intensity profile of the white line DL with the four-circle X-ray diffractometer installed on beam line BL-10A of the Photon Factory, National Laboratory for High Energy Physics. We used synchrotron radiation of wavelength 1·540 Å, monochromatized by the 111 reflection from a silicon crystal. The incident-beam slit set between the monochromator and the specimen was about 3 m from the (effective) X-ray source. Its cross section was 0·21 × 4·0 mm. The receiving slit at the detector was 250 mm from the specimen and its cross section was 0·2 × 6·0 mm.

To obtain the intensity profile of the diffuse scattering in which a white line is expected, constant-step-scanning measurements of the counter were made across the diffuse scattering with the specimen crystal fixed near the 200 Bragg position. Fig. 4 shows a measured profile of diffuse scattering plotted against the scattering angle (2θ) for the $\Delta\omega = -1°$. Here, intensity counts indicate the net data obtained by subtracting the background from raw data. The statistical error is shown with a bar on each datum point. A dip corresponding to the white line DL is observed about $2\theta = 49·1°$ in Fig. 4. The strongest peak is due to the tail of the 200 Bragg reflection from the crystal even when it is set far from its exact Bragg position.

We now estimate theoretically the intensity of DL in the symmetric Bragg geometry according to the treatment given by Bushuev & Lyubimov (1987) and Oya & Kashiwase (1988). The contrast factor R of

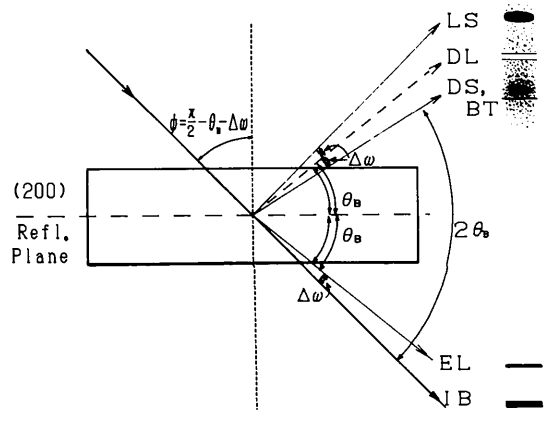

Fig. 3. Schematic illustration of the geometry of a diffraction pattern including the white line DL in the Bragg geometry. Diffuse scattering X-ray waves are reflected by the ($\bar{2}00$) net plane. Here ψ and θ_B are the incident and 200 Bragg reflection angles, respectively. Symbols in the figure are IB, incident beam; EL, black line; DS, intensity maximum point of diffuse scattering; LS, Laue spot.

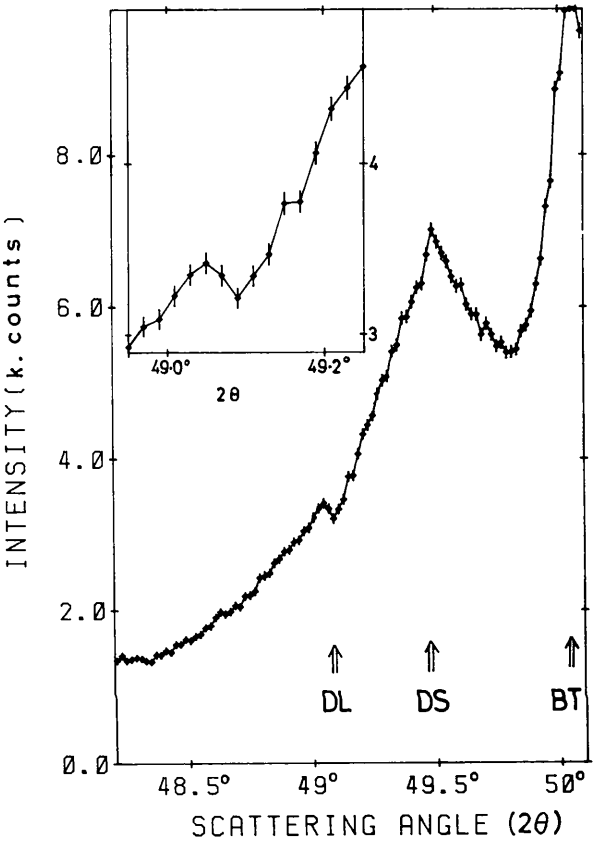

Fig. 4. Observed intensity profile, plotted against scattering angle (2θ) when $\Delta\omega = -1°$, corresponding to the white line DL across the 200 diffuse scattering of a Cu-Al disordered crystal. The intensity represents the net data obtained by subtracting the background, *not* the raw data. The statistical error is shown with a bar on each datum point. Inset shows the enlarged plots around the DL.

the DL is defined by

$$R=(I-I_0)/I_0,$$

where I is the intensity including the dip corresponding to DL and I_0 is the hypothetical intensity of diffuse scattering when the Bragg reflection does not occur. Assuming that $|\Delta\omega| \ll \theta_B$ and diffuse scattering intensity is negligibly small around the reciprocal-lattice origin in comparison with the reciprocal-lattice point, we have the contrast factor $R(x)$ given by

$$\begin{aligned}R(x)=\{&2(\rho+y+1)(1+2y)^{1/2}\exp(-\mu l_e)\\&+y^2[\exp(rl)-\exp(-rl)]\\&\times\{[1+y+(1+2y)^{1/2}]\exp(rl)\\&-[1+y-(1+2y)^{1/2}]\exp(-rl)\}^{-1}\\&\times 2/(\rho^2-2y-1)+\exp(-2\mu l_e)\}\\&\times[1-\exp(-2\mu l_e)]^{-1},\end{aligned}$$

with

$$y=y_0\exp(-x^2\ln 2),\quad x=\Delta\theta/\Delta\theta_B,$$

$$y_0=0{\cdot}47Q/\mu\Delta\theta_B,$$

$$\rho=-\sin\theta_B/\sin(\theta_B+\Delta\omega),\quad r=\mu(1+2y)^{1/2}/\sin\theta_B,$$

$$l_e=l/\sin\theta_B.$$

Here, l is the thickness of the specimen, μ is the linear absorption coefficient, $\Delta\theta=2\theta-2\theta_B-\Delta\omega$ and 2θ is the scattering angle. Q is the kinematical cross section per unit volume given as

$$Q=\left(\frac{e^2}{mc^2}\right)^2\frac{\lambda^3|F|^2}{v_a^2}\frac{1}{\sin 2\theta_B}P.$$

λ, F, v_a and P are wavelength, structure factor with Debye–Waller factor, unit-cell volume and polarization factor, respectively.

In the estimation of $R(x)$ for our Cu–Al alloy, we use the average scattering amplitude for the structure factor F, the average absorption coefficient as the linear absorption coefficient μ, and the observed value of HWHM = 3′ as the degree of perfection $\Delta\theta_B$ in the mosaic crystal. Since we have no value of the Debye–Waller factor for the sample, we must estimate this value where the displacement amplitude may be larger than that of pure Cu. However, we obtained the same contrast of DL within experimental error, using 1–2 times the pure Cu value.

As the diffuse scattering may be due to the several causes described above, it is difficult to calculate the angular dependence of hypothetical total diffuse intensity I_0. We tried to calculate the intensity of the first-order TDS in the long-wavelength approximation using the elastic constants of Cu–13·25 at.% Al alloy by Cain & Thomas (1971). The solid curve in Fig. 5(a) shows the curve of TDS, including the DL before resolution correction, when the maximum calculated intensity was fitted to the experimental maximum intensity. A dotted curve shows another TDS curve fitted around the DL with Fig. 4. These calculated curves both show a substantial difference from our experimented results. The calculated intensity distribution of TDS could therefore not explain the experimental angular dependence of the intensity of diffuse scattering. This calculated intensity is also confirmed using the results of the phonon dispersion relation of $Cu_{84}Al_{16}$ by Chou, Shapiro, Moss & Mostoller (1990).

Next, we estimate the intensity of DL using the experimental curve. A Lorentz distribution function fitted to the observed intensity in the region $48{\cdot}2 < 2\theta < 49{\cdot}4°$ except around DL was assumed as the intensity distribution of diffuse scattering. All components of diffuse scattering are included in this curve. Fig. 5(b) shows two fitted curves including the DL. The solid curve of Fig. 5(b) shows the diffuse scattering including the DL before resolution correction. A dotted curve shows the curve corrected by the convolution of resolution function and solid curve. Both calculated curves make only a slight difference in this experimental result using the very sharp slit system. By comparing the experimental curve of Fig. 4 and the dotted curve of Fig. 5(b), the two curves are seen to be in fair agreement. The experimental DL is sharper and slightly weaker than the calculated one. If this overestimation is induced in our thinking, the calculated DL will show stronger contrast and that is in poorer agreement with the experimental DL. Here, we probably overestimated the degree of misorientation of the perfect domains of the sample. One reason for reducing the contrast is underestimation of background, but this may not be crucial as judged by the trend of the observed intensity curves. A principal reason is perhaps the 'incoherent' scattering and diffuse scattering due to SRO in this intensity. This is discussed in the next section.

These results could be confirmed by an additional experiment using an Imaging Plate in which intensity can be read as digital data by each $0{\cdot}1\times 0{\cdot}1$ mm area (Amemiya, Matsushita, Nakagawa, Satow & Miyahara, 1988).

Discussion

The diffraction effect of diffuse scattering in a Cu–Al solid-solution crystal is summarized as follows.

(1) The white line, defect line (DL), a diffraction pattern caused by the $\bar{2}00$ Bragg reflection with extinction effect following the diffuse scattering, is observed in the diffuse scattering near the 200 reflection.

(2) The angles of the propagating direction of the DL from the BT and from the LS are equal to the corresponding offset angle $\Delta\omega$ from the exact Bragg position. The cause of the DL is in the quasi-elastic scattered X-rays, and not due to the inelastic X-rays

by Compton scattering. The effect of fluorescence was reduced to a negligibly small amount in this experiment using monochromatized or filtered Cu $K\alpha$ X-rays.

(3) In this solid-solution crystal, there exists considerable diffuse scattering due to the static displacement of atoms including the size-effect modulation of the SRO scattering and the Huang scattering in addition to TDS.

(4) The observed contrast of DL is quantitatively in fair agreement with the calculated one when the effect of static diffuse scattering is taken into account. This is related to the fact that the Huang diffuse scattering, due to the static displacement of atoms, behaves like TDS in producing DL, and the 'incoherent' scattering and diffuse scattering due to SRO are very weak.

(5) The DL is observed even at 3 ° and further from the exact Bragg position.

Finally, we briefly discuss the effect of diffuse scattering around the incident direction which is disregarded in the above treatment. It is there that the 'incoherent' scattering and diffuse scattering due to SRO do not depend on the wave vector, in contrast with TDS, and these are slightly stronger around lower-index reflections. The diffraction effect expected to be caused by this scattering is inclined to produce a very weak black line EL around the 200 reflection. This has the opposite effect on the contrast of the DL to that due to TDS and the Huang scattering. It should be noted that the existence of the diffuse intensity around the reciprocal-lattice origin affects the intensity distribution including the DL. Contribution of the scattering near the origin to the DL cannot be neglected in a detailed analysis. This is probably one of reasons why the experimental DL has a slightly weaker contrast than the calculated DL.

To clarify the diffraction effects of diffuse scattering due to static displacement of atoms in the solid-solution crystal, it is necessary to perform further experiments on the temperature dependence and much wider angle dependence including DL intensity measurements around other reflection points. The experiment should also be made using a solid solution

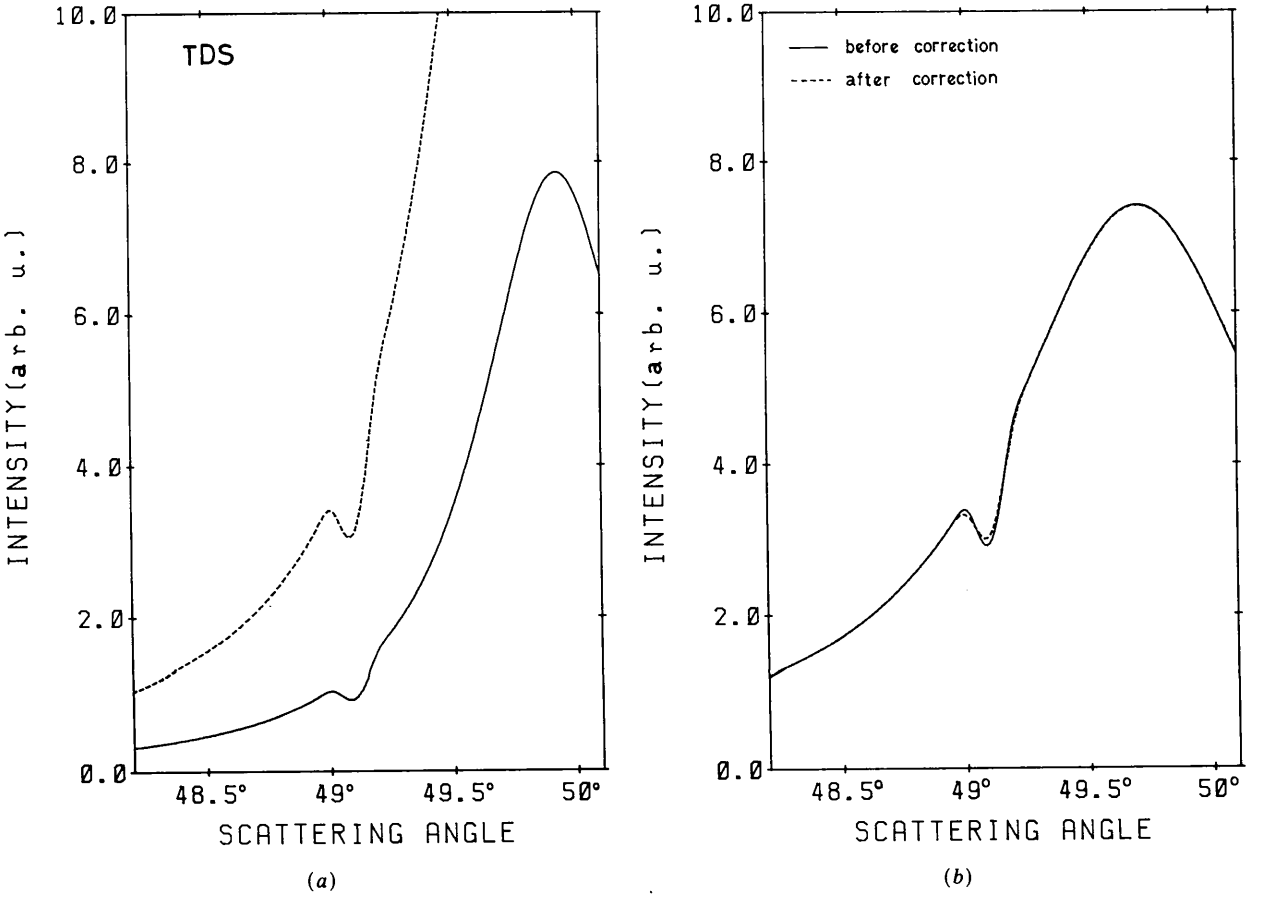

Fig. 5. Calculated curves for $\Delta\omega = 1°$ by using $\Delta\theta_B = 3'$ (observed half-angular-width at half-maximum) as the degree of perfection in a mosaic crystal. (*a*) The calculated TDS curves using the elastic constants of Cu-13·25 at.% Al alloy. The solid curve is fitted to the experimental result in Fig. 4 at the maximum intensity. The dotted curve is a scaling up of the solid line fitted around the DL in Fig. 4. (*b*) Semi-empirically calculated curves. The solid curve is not corrected and the dotted curve is corrected by the resolution function.

having a very small size effect such as an Au-Ag disordered alloy.

The authors thank Mr M. Minoura and Mr K. Ushida for their help. They also express their sincere thanks to Dr Y. Amemiya of the Photon Factory, National Laboratory for High Energy Physics. They are indebted to Dr S. C. Moss, University of Houston, for a critical reading of the manuscript.

References

AMEMIYA, Y., MATSUSHITA, T., NAKAGAWA, A., SATOW, Y. & MIYAHARA, J. (1988). *Nucl. Instrum. Methods*, **A266**, 645-653.
BUSHUEV, V. A., LAUSHKIN, A. V., KUZ'MIN, R. N. & LOBANOV, N. N. (1983). *Sov. Phys. Solid State*, **25**, 228-233.
BUSHUEV, V. A. & LYUBIMOV, A. G. (1987). *Sov. Phys. Crystallogr.* **32**, 179-184.
CAIN, L. S. & THOMAS, J. F. JR (1971). *Phys. Rev. B*, **4**, 4245-4255.
CHOU, H., SHAPIRO, S. M., MOSS, S. C. & MOSTOLLER, M. (1990). Submitted to *Phys. Rev. B*.
EPPERSON, J. E., FÜRNROHR, P. & ORTIZ, C. (1978). *Acta Cryst.* **A34**, 667-681.
HAMILTON, W. C. (1957). *Acta Cryst.* **10**, 629-634.
KAINUMA, Y. (1955). *Acta Cryst.* **8**, 247-257.
KAINUMA, Y. (1961). *J. Phys. Soc. Jpn*, **16**, 228-241.
KASHIWASE, Y., KAINUMA, Y. & MINOURA, M. (1981). *J. Phys. Soc. Jpn*, **50**, 2793-2794.
KASHIWASE, Y., KAINUMA, Y. & MINOURA, M. (1982). *Acta Cryst.* **A38**, 390-391.
KASHIWASE, Y., MORI, M., KOGISO, M., MINOURA, M. & SASAKI, S. (1988). *J. Phys. Soc. Jpn*, **57**, 524-534.
KASHIWASE, Y., MORI, M., KOGISO, M., USHIDA, K., MINOURA, M., ISHIKAWA, T. & SASAKI, S. (1989). *Phys. Rev. Lett.* **62**, 925-928.
OYA, Y. & KASHIWASE, Y. (1988). *J. Phys. Soc. Jpn*, **57**, 2026-2039.
WARREN, B. E. (1969). *X-ray Diffraction*, Ch. 12. Reading, MA: Addison-Wesley.
ZACHARIASEN, W. H. (1967). *Acta Cryst.* **23**, 558-564.

Acta Cryst. (1990). **A46**, 929-934

Direct Methods in Superspace. II. The First Application to an Unknown Incommensurate Modulated Structure*

BY XIANG SHI-BIN, FAN HAI-FU,† WU XIAO-JING AND LI FANG-HUA

Institute of Physics, Chinese Academy of Sciences, Beijing 100080, *People's Republic of China*

AND PAN QING

Structure Research Laboratory, University of Science and Technology of China, Hefei 230026, *People's Republic of China*

(*Received* 16 *February* 1990; *accepted* 28 *June* 1990)

Abstract

The direct method previously proposed [Hao, Liu & Fan (1987). *Acta Cryst.* **A43**, 820-824] has been used to determine the incommensurate modulation in the structure of ankangite by using the $h0l$ electron diffraction pattern. Ankangite is a newly discovered mineral which belongs to the priderite group with chemical composition $Ba_{0.8}(Ti, V, Cr)_8O_{16}$. The $h0l$ electron diffraction pattern shows sharp satellite reflections which correspond to a one-dimensional incommensurate modulation along the c axis. Direct phasing of the $h0l$ satellite reflections based on the known phases of the main reflections led to a three-dimensional hyperprojection along the a_2 direction of the four-dimensional electron potential distribution, revealing clearly occupational and positional modulations of the Ba atoms. Positional modulation of other atoms has also been observed.

Introduction

The purpose of the present study is threefold:

(1) Ankangite $Ba_{0.8}(Ti, V, Cr)_8O_{16}$ is a newly found mineral belonging to the priderite group (Xong, Ma & Peng, 1984). Electron-microscopy studies found that the mineral is an incommensurate modulated phase. A prediction for the form of modulation has also been made qualitatively based on electron diffraction patterns and high-resolution electron micrographs (Wu, Li & Hashimoto, 1990). A quantitative determination of the incommensurate modulation is useful for better understanding of the structure.

(2) Recently, a direct method has been proposed for solving incommensurate modulated structures (Hao, Liu & Fan, 1987, hereafter referred to as paper I). Unlike the others, this method does not rely on any assumption about the property of modulation. It

* Supported by the National Natural Science Foundation of China.

† To whom all correspondence should be addressed.

0108-7673/90/110929-06$03.00